

# Computer simulation of neural networks for perceptual psychology

STEPHEN GROSSBERG and ENNIO MINGOLLA  
*Center for Adaptive Systems, Boston University, Boston, Massachusetts*

Computer simulations of neural network processes fill an important methodological niche, permitting the investigation of questions not resolvable by physiological, behavioral, or formal approaches alone. Two types of network simulations are considered: simulations of boundary completion and simulations of segmentation. Simulations that compare properties of published models with variations of these models are presented to illustrate how parametric computer simulations have guided the development of neural models of visual perception.

## The Role of Computer Simulations in Theory Development

The dynamics of large ensembles of neurons are as yet difficult to observe directly. Even if direct observation were possible, it would not explain how the interactions among neurons generate the emergent properties that subserve intelligent behavior. Additional methodologies are needed to investigate how the collective properties of a neural network are related to its components. Computer simulations of neural networks are crucial tools in the current explosion of work in brain science. Although anatomical, physiological, and behavioral methods continue to be fundamental, theoretical investigations of perceptual, cognitive, and motor tasks are gaining increasing importance, thanks in part to the ability afforded by computers to implement and test formal models of distributed brain processes.

Many basic problems of skilled behavior can now be modeled in sufficiently precise terms to permit formal mathematical investigation. Once a mathematical model of neural functioning is formulated, the investigation of its properties may culminate in the proof of theorems concerning the stability or convergence behavior of the model, as in Cohen and Grossberg (1983). Certain classes of models of neurally based processes, however, particularly those involving large and hierarchically organized systems of nonlinear ordinary differential equations, are characteristically difficult to analyze through purely formal procedures. For these systems there may be no way to determine the output of the model when given a certain input, short of running the model in a numerical computer simulation. Thus, "experiments" can be run on a

---

Stephen Grossberg's work was supported in part by the Air Force Office of Scientific Research (AFOSR 85-0149 and AFOSR F49620-86-C-0037), the Army Research Office (ARO DAAG-29-85-K-0095), and the National Science Foundation (NSF IST-84-17756). Ennio Mingolla's work was supported in part by the Air Force Office of Scientific Research (AFOSR 85-0149). We wish to thank Cynthia Suchta for her valuable assistance in the preparation of the manuscript and illustrations. Address correspondence to Ennio Mingolla, Center for Adaptive Systems, Boston University, 111 Cummington Street, Boston, MA 02215.

model in ways that are similar in some respects to experiments run on human or animal subjects.

Models, by definition, do not contain all the richness of the biological processes they model; their very explanatory power comes in part from their greater simplicity. Nevertheless, once the component mechanisms of a model are known to be qualitatively valid, computer simulations have certain distinct advantages over experiments on actual organisms. Simulations can be cheaper and faster, but more importantly, they permit a much more precise level of control of many variables than could ever be realized in physiological or behavioral experimental paradigms. Thus, parameters in a model can be perturbed, or entire components of the model can be deleted or replaced with other mechanisms, by changing the appropriate parts of computer programs. Such systematic investigations can yield a deeper appreciation of the modeled mechanisms and their variants, both normal and abnormal; suggestions for corroborative experiments on live organisms; and even general design insights that can, at times, be formalized into mathematical proofs that would otherwise have been difficult to discover.

## Simulation of a Neurally Based Model of Boundary Completion

This article presents two examples of the way in which performing computer simulations has helped the development of a perceptual theory, whose formal equations are listed in the Appendix. As these examples illustrate, each of the processing stages used in the model is essential for generating its formal perceptual properties. In this limited sense, at least, the model is a *minimal* model of the properties that it sets out to explain.

The first example involves variations of simulations that were first presented by Grossberg and Mingolla (1985a), who examined certain problems in boundary detection and completion faced by mammalian visual systems. Early visual processing by orientationally tuned, contrast-driven cells necessarily involves problems of positional and orientational uncertainty. For example, the very elongation of cell receptive fields (masks) necessary for preferen-

tial responses to oriented contrasts along straight luminance borders implies attenuated responses by these receptive fields at line ends and corners, as indicated in Figure 1. We summarize this property in terms of an uncertainty principle, namely, that *orientational certainty implies positional uncertainty at line ends and corners*. Figure 2 shows a computer simulation depicting this uncertainty at a line end.

According to our theory, the spatial pattern of early boundary detection signals depicted in Figure 2 requires subsequent processing whereby the positional uncertainty at line ends and corners is overcome. To this end, the mask responses in Figure 2 act as an input pattern to a later processing stage that preserves the strong responses at the line's long edges, but also completes the representation of the line at its end (Grossberg & Mingolla, 1985a, 1985b). We call the emergent pattern of activity at the end of a line an *end cut*, an example of which is shown in Figure 3.

The processing stages that are hypothesized to generate end cuts are summarized in Figure 4. These processing stages have also been used to analyze a wide variety of perceptual and neural data (Grossberg, in press a, in

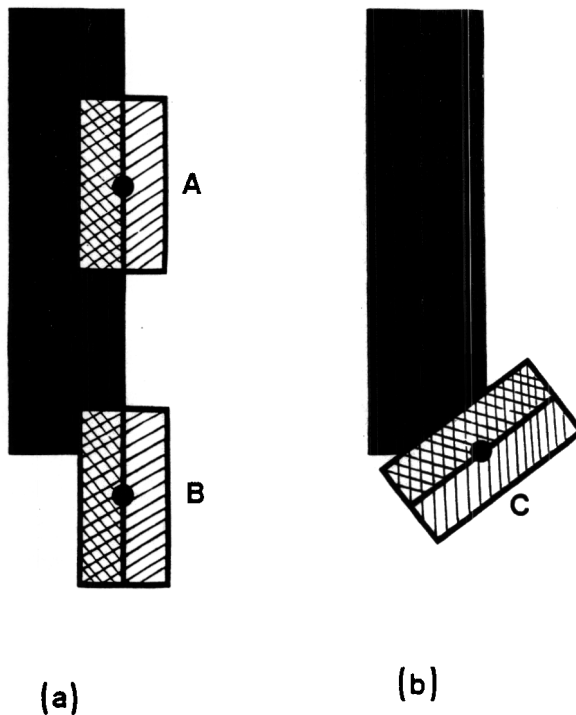


Figure 1. Orientational specificity at figural edges, corners, and exteriors. (a) At positions that are along a figural edge but not at a figural corner, such as A, the oriented mask parallel to the edge is highly favored. At positions beyond the edge, such as B, masks of the same orientation are still partially activated. This tendency can, in the absence of compensatory mechanisms, support a flow of dark featural activity down and out of the black figure. (b) A line is thin, functionally speaking, when at positions near a corner, such as C, many masks of different orientations are all weakly activated or not activated at all.

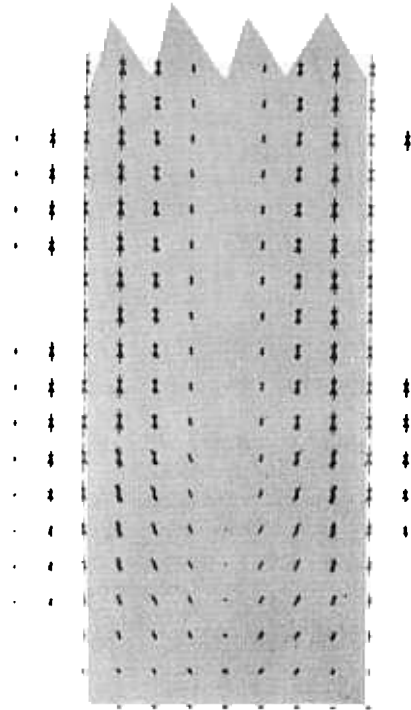


Figure 2. An orientation field: Lengths and orientations of lines encode the relative sizes of the activations and orientations of the input masks at the corresponding positions. The input pattern, which is a vertical line end as seen by the receptive fields, corresponds to the shaded area. Each mask has total exterior dimensions of  $16 \times 8$  units, with a unit length being the distance between two adjacent lattice positions.

press b; Grossberg & Mingolla, 1985a, 1985b, in press). First, oriented receptive fields of like position and orientation but opposite direction of contrasts, cooperate at the next processing stage to activate cells whose receptive fields are sensitive to the same position and orientation as themselves, but which are insensitive to direction of contrast. These target cells maintain their sensitivity to the *amount* of oriented contrast, but not to the *direction* of this oriented contrast. The computer simulation summarized in Figure 2 depicts the responses of cells at this processing stage. Such model cells, which play the role of complex cells in Area 17 of the visual cortex, pool inputs from receptive fields with opposite directions of contrast in order to generate boundary detectors that can detect the broadest possible range of luminance or chromatic contrasts (Grossberg, in press a; Thorell, DeValois, & Albrecht, 1984). These two successive stages of oriented contrast-sensitive cells are called the *OC filter* (Grossberg & Mingolla, 1985b).

The output from the OC filter successively activates two types of short-range competitive interaction, whose net effect is to generate end cuts. First, a cell of prescribed orientation excites like-oriented cells corresponding to its location and inhibits like-oriented cells corresponding to

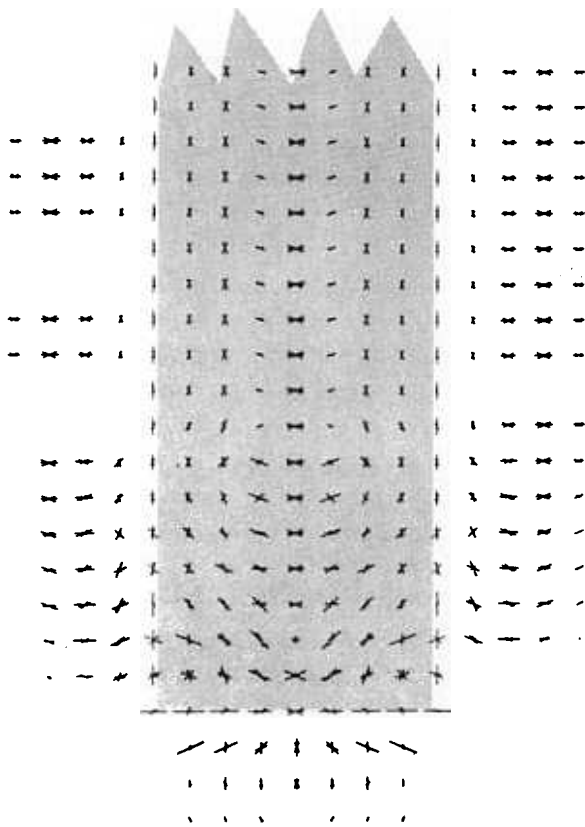


Figure 3. Responses of a network with two stages of short-range competition to the orientation field of Figure 2: A process called *end cutting* generates horizontal activations at line end locations that receive small and orientationally ambiguous input activations.

nearby locations at the next processing stage. In other words, an on-center off-surround organization of like-oriented cell interactions exists around each perceptual location. The outputs from this competitive mechanism interact with the second competitive mechanism. Here, cells compete that represent different orientations, notably perpendicular orientations, at the same perceptual location. This competition defines a push-pull opponent process. If a given orientation is excited, then the perpendicular orientation at its location is inhibited. If a given orientation is inhibited, then the perpendicular orientation at its location is excited via disinhibition.

These competitive rules generate end cuts as follows. The strong vertical activations along the edges of a scenic line, as in Figure 2, inhibit the weak vertical activations near the line end. These inhibited vertical activations, in turn, disinhibit horizontal activations near the line end, as in Figure 3. Thus the positional uncertainty at line ends that is caused by orientational tuning is eliminated by the interaction of two short-range competitive mechanisms.

The properties of the two stages of competition can be formally dissected through the use of simulations that omit one or the other stage. Figure 5 shows the effects of feeding signals proportional to the output of oriented masks

directly to the second competitive stage; thus the first competitive stage is eliminated and the mask field pattern shown in Figure 2 is input directly to the second competitive stage. Figure 6, conversely, shows the output of the first competitive stage to the input signal pattern shown in Figure 2. Together, Figures 5 and 6 illustrate the importance of coupling the two successive competitive stages. Without the first competitive stage (Figure 5), the output pattern has a broad band of vertically oriented activity along the sides of the line, thereby failing to adequately localize the sides of the line itself. Without the second competitive stage (Figure 6), almost all signals are swamped by noise.

### Implementation of Simulations Using Algebraic Equations

Simulations of the kind shown in Figure 2 are relatively easy to perform, in terms of both programming difficulty and computer processing time, because they involve only algebraic calculations of contrast distributions in an image. (See Appendix, Equation A1.) In image processing terms, one performs a convolution of the image with

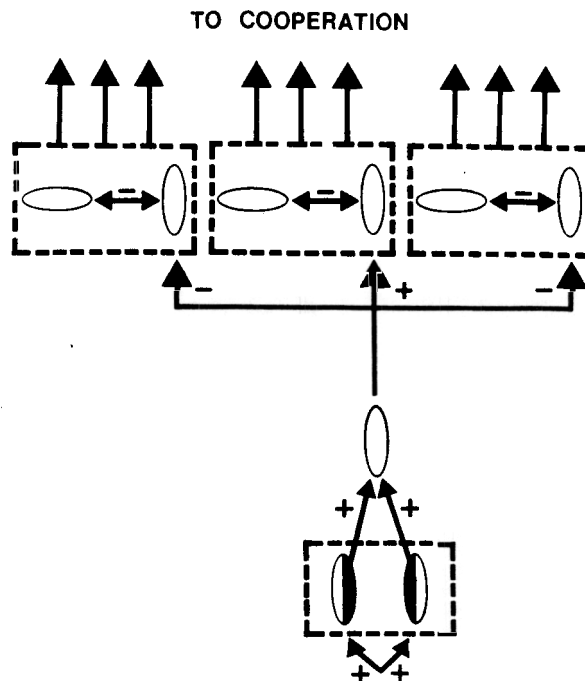


Figure 4. Early stages of boundary contour processing: At each position exist cells with elongated receptive fields of various sizes that are sensitive to orientation, amount of contrast, and direction of contrast. Pairs of such cells that are sensitive to like orientation but to opposite directions of contrast (lower dashed box) input to cells that are sensitive to orientation and amount of contrast but not to direction of contrast (white ellipses). These cells, in turn, excite like-oriented cells corresponding to the same position and inhibit like-oriented cells corresponding to nearby positions at the first competitive stage (upper dashed boxes). At this stage, cells corresponding to the same position but to different orientations inhibit each other via a push-pull competitive interaction.

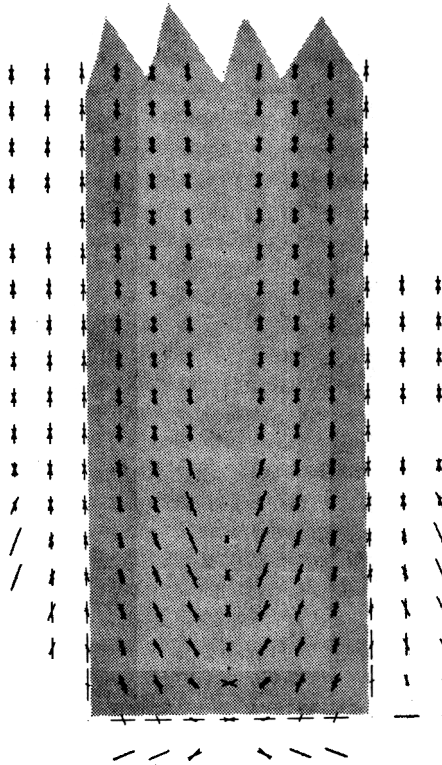


Figure 5. This simulation was performed with the second competitive stage responding directly to the inputs of the orientation field in Figure 2, without any processing by the first competitive stage. The sides of the line (indicated by the shaded region) are not well localized by the network.

oriented kernels (weighting functions) that express the oriented contrast sensitivity of masks. The difference between an ordinary image convolution and the simulation shown in Figure 2, is that, in the latter, only a sparse lattice of image locations is sampled in order to form the grid of mask responses over several orientations, and the larger of the two convolutions is plotted at each location and orientation to implement the insensitivity of the masks to direction of contrast, as defined in the numerator of Equation A1 of the Appendix.

Simulations such as those shown in Figures 3, 5, and 6 are also easy to perform, since they also can be executed using only algebraic equations. The networks involved in the simulation of Figure 3 are defined by a system of Equations A1 through A6 of the Appendix. These equations represent a feedforward flow of activation from the input masks to the competitive stages. The equilibrium states of this system can therefore be easily computed. In fact, all equations but A4 are already computed at equilibrium. The equilibrium of A4 can be computed simply by setting the rate of change,  $(d/dt)w_{ijk}$ , of  $w_{ijk}$  equal to zero. Thus, at equilibrium,

$$w_{ijk} = \frac{I + BJ_{ijk} + v_{ijk}}{1 + B \sum_{(p,q)} J_{pqk} A_{pqij}} \quad (1)$$

For the simulations of Figures 3, 5, and 6, all  $v_{ijk}$ s are set identically equal to zero, since no feedback is involved. The simulations shown in Figures 5 and 6 were performed by replacing Equations 1 and A6 by

$$w_{ijk} = I + BJ_{ijk} \quad (2)$$

and

$$y_{ijk} = w_{ijk}, \quad (3)$$

respectively. All other relevant equations and quantities were identical to those used for the simulation shown in Figure 3.

### Simulation of Textural Segmentation and Perceptual Grouping

The second set of simulations concerns the role of long-range cooperative activity among oriented cells at a processing stage subsequent to the two short-range competitive stages. In our theory, this cooperation is crucial to the understanding of boundary detection and completion, textural segmentation and grouping, surface per-

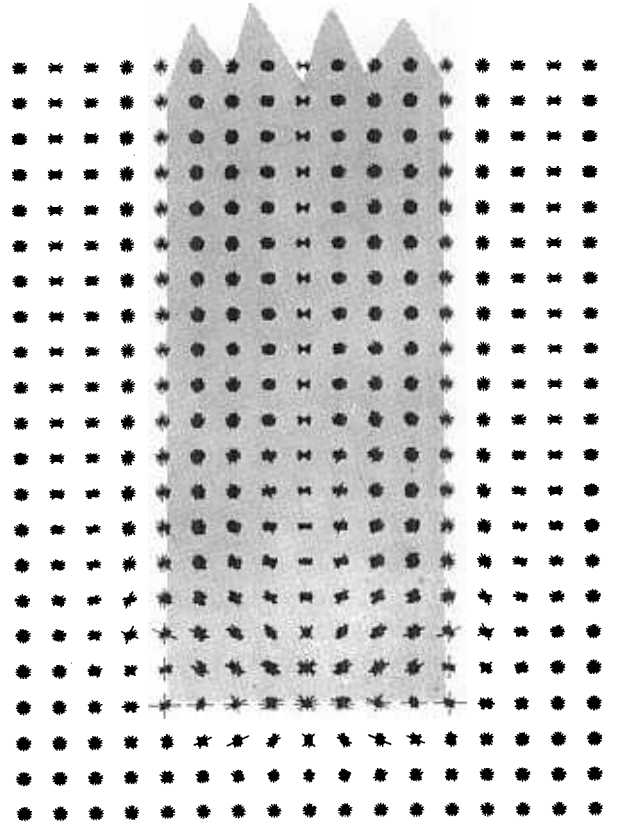


Figure 6. Responses of the first competitive stage to the input of the orientation field in Figure 2. Without processing by the second competitive stage, almost all responses to the line (indicated by the shaded region) are swamped by noise.

ception, and the perception of illusory contours (Grossberg & Mingolla, 1985b, in press). The cooperation is mediated by oriented cells with two separately thresholded receptive fields, as indicated in Figure 7. The alignment of the two receptive field weighting functions is such that, for example, a horizontally oriented cooperative cell tends to fire whenever it receives sufficiently strong signals from approximately horizontally oriented cells of the second competitive stage to both receptive fields simultaneously. When the cooperative cell fires, it sends excitatory signals back to the similarly oriented cells corresponding to its position at the first competitive stage, and inhibitory signals to similarly oriented cells corresponding to nearby positions. These top-down signals set up a feedback loop between the long-range cooperative process and the short-range competitive processes. This cooperative-competitive feedback process is called the CC loop. The design constraints leading to the entire system for implementing the CC loop are beyond the scope of this article, and can be found in Grossberg and Mingolla (1985b). The role of computer simulations in the formulation of one key functional capacity of the CC loop is instead described in detail.

Figure 8 presents the results of two separate simulations of textural grouping. Figure 8a shows the input pattern that is presented to the CC loop. The pattern consists of nine clusters of 18 vertically oriented mask responses. We call each cluster a Line because it is a caricature of how a finer lattice of masks would respond to an actual line. Figure 8b displays the pattern of equilibrium activities that is generated by this input at the second competitive stage of the full model, including CC loop feedback. This simulation is a success because, without any preassigned template or external prompting, the network has automatically regulated itself to an equilibrium state wherein each Line, besides being surrounded by its own boundary activity, is also emergently grouped with neighboring vertical and horizontal Lines in a manner similar to that found in human perception (see Beck, Prazdny, & Rosenfeld, 1983, for an excellent review).

**The Postulate of Spatial Impenetrability**

Because the only inputs for the simulation summarized in Figure 8b were the vertical activities shown in Figure 8a, it is clear that the emergent horizontal groupings came about through horizontal cooperative activity induced by horizontal end cut signals that are generated at the ends of Lines by the second competitive stage. If such horizontal end cuts induce horizontal groupings at line ends, however, why do the horizontal signals induced along the sides of the Lines not also group, thereby flooding the entire region between Lines with activity? Precisely this event is shown in Figure 8c, which shows the results of a simulation run not on our actual model but on a variation of it.

Our actual CC loop model (Figure 7b) avoids the disaster shown in Figure 8c by instantiating a computational property that implements what we have termed the *postu-*

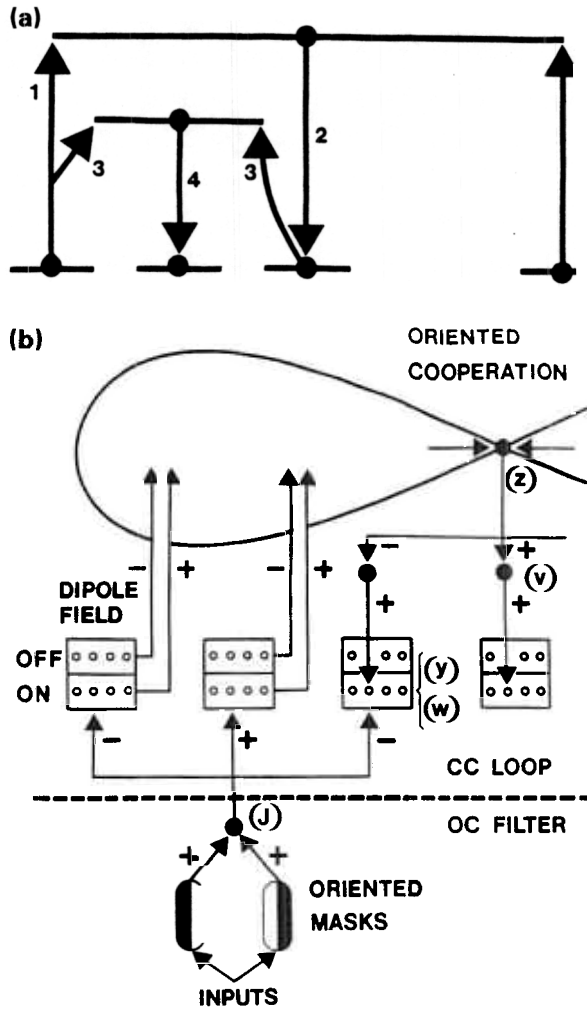


Figure 7. An overview of cooperative feedback. (a) The pair of pathways 1 activate positive boundary completion feedback along pathway 2. Then pathways such as 3 activate positive feedback along pathways such as 4. Rapid completion of a sharp boundary between the locations of pathways 1 can hereby be generated by a spatially discontinuous bisection process. (b) Circuit diagram of the Boundary Contour System: Inputs activate oriented masks, which cooperate at each position and orientation before feeding into an on-center off-surround interaction. This interaction excites like-oriented cells at the same position and inhibits like-oriented cells at nearby positions. The affected cells are on-cells within a dipole field. On-cells at a fixed position compete among orientations. On-cells also inhibit off-cells that represent the same position and orientation. Off-cells at each position, in turn, compete among orientations. Both on-cells and off-cells are tonically active. Net excitation of an on-cell excites a similarly oriented cooperative receptive field at a location corresponding to that of the on-cell. Net excitation of an off-cell inhibits a similarly oriented cooperative receptive field of a bipole cell at a location corresponding to that of the off-cell. Thus, bottom-up excitation of a vertical on-cell, by inhibiting the horizontal on-cell at that position, disinhibits the horizontal off-cell at that position, which in turn inhibits (almost) horizontally oriented cooperative receptive fields that include its position. Sufficiently strong net positive activation of both receptive fields of a cooperative cell enables the cell to generate feedback via an on-center off-surround interaction among like-oriented cells. On-cells that receive the most favorable combination of bottom-up signals and top-down signals generate the emergent perceptual grouping. The letters in this figure are keyed to the variables in the Appendix.

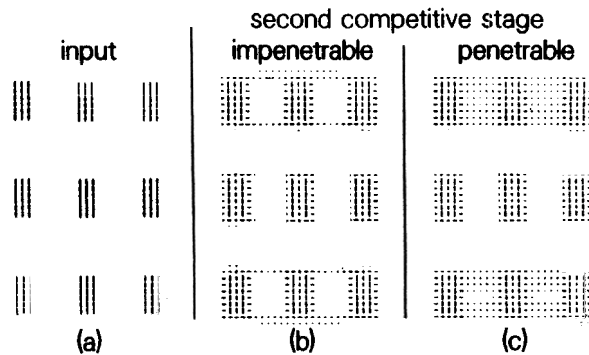


Figure 8. Computer simulations of processing underlying textural grouping. The length of each line segment is proportional to the activation of a network node responsive to one of 12 possible orientations. Part (a) displays the activity of oriented cells that input to the CC loop. Part (b) displays the groupings sensed by our actual model network. Part (c) displays the resulting flooding of boundary activity that occurs when the model's mechanism for spatial impenetrability is removed. See text for details of the two simulations shown in (b) and (c).

*late of spatial impenetrability.* This postulate acknowledges the need to prevent the cooperative process from being able to leap across, and thereby penetrate, all intervening percepts. Figure 9 motivates the mechanisms that we have developed to implement the postulate of spatial impenetrability. Figure 9 shows the left halves of the receptive fields of two horizontally tuned cooperative cells. In our actual model, horizontal activations at the second competitive stage that fall within such a horizontally tuned cooperative cell's receptive field generate excitatory inputs to the receptive field. Vertical activations, in contrast, generate inhibitory inputs to the receptive field. (The pairing of excitatory and inhibitory inputs at perpendicular orientations is represented by the terms  $y_{pqr} - y_{pqr}$  in Equation A7.) Thus, by summing excitatory and inhibitory inputs from the second competitive stage, the left receptive field of the lower cooperative cell of Figure 9 can be excited above threshold, because of the preponderance of horizontals from the end cut. On the other hand, the upper cooperative cell's left receptive field receives net inhibition because signals from the six vertical segments overwhelm those from the four horizontals. Our neural model of how both excitatory and inhibitory signals input to a cooperative cell assumes that on-cells generate the excitatory inputs and off-cells generate the inhibitory inputs from the second competitive stage. These cells, taken together, are called a dipole field, as illustrated in Figure 7b.

The model variation whose noisy output is shown in Figure 8c was achieved by removing the inhibitory effects of signals oriented orthogonally to the cooperative cell's preferred orientation ( $-y_{pqr}$ ) while keeping the excitatory effects of signals at the same orientation as the cooperative cell itself ( $y_{pqr}$ ). Indeed, along with study of perceptual and physiological data and earlier theoretical results, observation of simulations such as that shown in

Figure 8c played a crucial role in our development of the CC loop model in its present form.

### Implementation of Perceptual Grouping Simulations

Performing the simulations of Figure 8 involves more complexity than is apparent from the output displays themselves. For example, the lattice of network nodes contains 12 orientations at each of  $40 \times 25$  spatial locations for five network processing stages. This means that 60,000 nonlinear ordinary differential equations must be solved to perform each of the simulations in Figure 8. One factor prevents the computational demands from being completely unmanageable: Some of the equations can be solved algebraically, in the same manner as those for the end cut simulations (Figure 3). Because the full model involves feedback, however, the use of algebraic approximations requires explicit assumptions about reaction rates within the model. That is, those stages whose equilibria are computed algebraically are assumed to equilibrate more rapidly than do the other stages. The Appendix describes which equations were solved algebraically and which were solved through numerical integration.

For the simulations of Figure 8, the numerical integration of the differential equations not solved algebraically was carried out using the DGEAR subroutine package of the IMSL Library, which is commonly available at university computational facilities. Using IMSL is not much more difficult than using the packages for statistical anal-

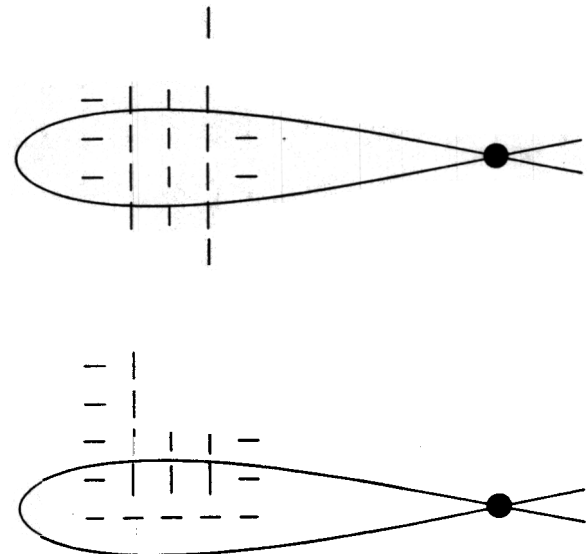


Figure 9. A mechanism to implement the postulate of spatial impenetrability: The left receptive fields of two horizontally tuned cooperative cells are crossed by a thin vertical line. Although horizontal end-cut signals can excite the upper receptive field, these are cancelled by the greater number of inhibitory inputs due to the vertical line inputs. Within the lower receptive field, the excitatory inputs due to end cuts prevail.

ysis so familiar to psychologists. Solving systems of simultaneous nonlinear differential equations, however, is notoriously slow work for general-purpose digital computers. The simulations of Figure 8, for example, took hours of computer time on a large IBM mainframe.

Those of us working on neurally based network models hope that the forthcoming generation of massively parallel hardware can be used to speed up simulations for basic research. Certain prototypes of parallel processors have in fact been developed along lines suggested by theoretical research on neural models that has been performed over the past two decades. In particular, TRW's new Mark III and Mark IV computers are designed to rapidly integrate a wide range of neural models at relatively low cost. We hope that this type of cooperative feedback loop between computer simulation and hardware development will speed the attainment both of theoretical understanding of biological processes and of development of advanced parallel hardware designs.

REFERENCES

BECK, J., PRAZDNY, K., & ROSENFELD, A. (1983). A theory of textural segmentation. In J. Beck, B. Hope, & A. Rosenfeld (Eds.), *Human and machine vision*. New York: Academic Press.

COHEN, M. A., & GROSSBERG, S. (1983). Absolute stability of global pattern formation and parallel memory storage by competitive neural networks. *IEEE Transactions, SMC-13*, 815-826.

GROSSBERG, S. (in press a). Cortical dynamics of three-dimensional form, color, and brightness perception: I. Monocular theory. *Perception & Psychophysics*.

GROSSBERG, S. (in press b). Cortical dynamics of three-dimensional form, color, and brightness perception: II. Binocular theory. *Perception & Psychophysics*.

GROSSBERG, S., & MINGOLLA, E. (1985a). Neural dynamics of form perception: Boundary completion, illusory figures, and neon color spreading. *Psychological Review*, **92**, 173-211.

GROSSBERG, S., & MINGOLLA, E. (1985b). Neural dynamics of perceptual grouping: Textures, boundaries, and emergent segmentations. *Perception & Psychophysics*, **38**, 141-171.

GROSSBERG, S., & MINGOLLA, E. (in press). Neural dynamics of surface perception: Boundary webs, illuminants, and shape-from-shading. *Computer Vision, Graphics, & Image Processing*.

THORELL, L. G., DEVALOIS, R. L., & ALBRECHT, D. G. (1984). Spatial mapping of monkey VI cells with pure color and luminance stimuli. *Vision Research*, **24**, 751-769.

APPENDIX

The following neural network equations represent the OC filter and the CC loop. All processes, except the first competitive stage, are assumed to react so quickly that they can be represented at equilibrium as algebraic equations. This approximation is merely a computational convenience to speed up the simulations, and does not influence the results. See Grossberg and Mingolla (1985b) for complete definitions of the network processes.

In all of the subsequent equations, indices  $(i,j)$  represent a cell

position within a two-dimensional lattice and  $k$  represents an orientation.

OC Filter

Complex Cell Receptive Fields

Letting  $S_{pq}$  equal the input to position  $(p,q)$ ,

$$J_{ijk} = \frac{[U_{ijk} - \alpha V_{ijk}]^+ + [V_{ijk} - \alpha U_{ijk}]^+}{1 + \beta(U_{ijk} + V_{ijk})} \tag{A1}$$

where

$$U_{ijk} = \sum_{(p,q) \in L_{ijk}} S_{pq}, \tag{A2}$$

$$V_{ijk} = \sum_{(p,q) \in R_{ijk}} S_{pq}, \tag{A3}$$

and the notation  $[p]^+ = \max(p,0)$ . In Equation A1, the elongated receptive field is divided into a left half  $L_{ijk}$  and a right half  $R_{ijk}$ .

CC Loop

First Competitive Stage

$$\frac{d}{dt} w_{ijk} = -w_{ijk} + I + B J_{ijk} + v_{ijk} - B \sum_{(p,q)} J_{pqk} A_{pqij}. \tag{A4}$$

Second Competitive Stage

$$O_{ijk} = C[w_{ijk} - w_{ijk}]^+, \tag{A5}$$

$$y_{ijk} = \frac{E O_{ijk}}{D + O_{ijk}}, \tag{A6}$$

where  $K$  is the orientation perpendicular to  $k$ , and  $O_{ij} = \sum_{k=1}^K O_{ijk}$ .

Cooperation

$$z_{ijk} = g\left(\sum_{(p,q,r)} [y_{pqr} - y_{pqr}] F_{pqij}^{(r,k)}\right) + g\left(\sum_{(p,q,r)} [y_{pqr} - y_{pqr}] G_{pqij}^{(r,k)}\right), \tag{A7}$$

where

$$g(s) = \frac{H[s]^+}{K + [s]^+} \tag{A8}$$

and kernels  $F_{pqij}^{(r,k)}$  and  $G_{pqij}^{(r,k)}$  define the cell's two receptive fields.

Cooperative Feedback to First Competitive Stage

$$v_{ijk} = \frac{h(z_{ijk})}{1 + \sum_{(p,q)} h(z_{pqk}) W_{pqij}} \tag{A9}$$

where

$$h(s) = L[s - M]^+. \tag{A10}$$